Neurocomputing 401 (2020) 271–280

Contents lists available at ScienceDirect

Neurocomputing

journal homepage: www.elsevier.com/locate/neucom

A closed-loop BMI system design based on the improved SJIT model and the network of Izhikevich neurons☆

Hongguang Pan[a,b], Wenyu Mi[a], Xinyu Lei[a], Weimin Zhong[b,*]

[a] College of Electrical and Control Engineering, Xi'an University of Science and Technology, Xi'an 710054, China
[b] Key Laboratory of Advanced Control and Optimization for Chemical Processes, Ministry of Education, East China University of Science and Technology, Shanghai 200237, China

ARTICLE INFO

Article history:
Received 26 February 2019
Revised 27 October 2019
Accepted 16 March 2020
Available online 28 March 2020

Communicated by Dr. Nianyin Zeng

Keywords:
Brain–machine interface
Model improvement
Model predictive control
Closed-loop system design
Intracortical micro-stimulation

ABSTRACT

Brain–machine interface (BMI) is a useful technology which creates a new way for disable people to communicate with the world, but experimenting with human brains is risky. Hence, a precise mathematical model of the information transmission in the process of limb movement is necessary to be established. In this paper, firstly, we improve the classical single-joint information transmission (SJIT) model through introducing several neuron models, and the improved model is closer to the true single-joint movements. Secondly, a closed-loop system with a Wiener filter-based decoder, an auxiliary controller based on model predictive control (MPC) and a network of Izhikevich neurons is formulated based on the improved model, and the used network of Izhikevich neurons is more time efficient than the existing one. Finally, in this closed-loop system, the intracortical micro-stimulation (ICMS) technology is introduced to feedback the information from the MPC controller in real time. The auxiliary controller assist the brain to control artificial arm by changing the frequency of stimulation current. In this way, the computational complexity of the optimization problem proposed in this paper is greatly reduced, and the closed-loop BMI system designed in this paper can well track the desired trajectory.

1. Introduction

Brain–machine interface (BMI), as an emerging interdisciplinary technology, has developed rapidly in recent years [1–5]. It creates a new way to assist the brain communicate with external without relying on spine and muscle[1]. As a practical technology, BMI is widely used in the medical field such as the functional recovery of the movement for disabled people and the support for the elderly [6–8]. Generally, the BMI includes three parts: the decoder, the encoder and the measurement of neural activities in the cerebral cortex. Among them, when it is used in the functional recovery of joint movement, the decoder conveys the movement intention from the brain to the external device and the encoder feeds the motor information back to the brain [2]. A BMI system can be formulated by the BMI, brain and external device (such as the artificial arm).

Establishing a proper mathematical model for the information transmission in the process of limb movement is significant for studying BMI system [9–12]. In recent years, many studies have established or applied these kinds of mathematical models. Among them, Pollok et al. have analysed the basic principle about how the brain control fingers to move repeatedly in detail, which based on the qualitative relationship between brain regions S1/M1 and finger tapping activity [13]; based on the neural-network-based model used in [14], Esposti et al. have mentioned that the introduction of the feedback control is benefit to the reaching of limb in BMI system [14]; based on the single-joint information transmission (SJIT) model, Kumar et al. have designed a closed-loop BMI system [2,15]. Among these models, the SJIT model which proposed by Bullock et al. in 1998 has received much attention [2,15,16]. The main reasons are as follows: 1) the model depicts the mathematical relationship between the movement of arm joints and neurons in the brain area 4 and 5, which is easy to be used in theoretical research; 2) the model output is close to the actual output of human single-joint movement. Nevertheless, the SJIT model is not flawless. To facilitate the problem descriptions, this model can been seen as a system with a controller (the brain), and the limb

☆ This work is supported by the National Science Foundation of China (61603295), Outstanding Youth Science Fund of Xi'an University of Science and Technology (2018YQ2-07), Shaanxi postdoctoral Science Foundation (2018BSHEDZZ124), China Postdoctoral Science Foundation (2017M623207), and Natural Science Basic Research Plan in Shaanxi Province(2018JM6003).

* Corresponding author.
E-mail addresses: hongguangpan@163.com (H. Pan), wenyu_mi@163.com (W. Mi), leixinyu7879@163.com (X. Lei), wmzhong@ecust.edu.cn (W. Zhong).

https://doi.org/10.1016/j.neucom.2020.03.047
0925-2312/

position as the system output. The problem in this system is that the system overshoot is large. Considering this phenomenon does not happen in actual human movement, and a large overshoot will enhance the environmental requirements of the devices in practical applications, therefore, it is necessary to improve the performance of the SJIT model.

In recent years, there have been many studies on the formulation of the BMI system. According to these studies, the signal from the brain is changing during the limb movement, which makes it difficult for the BMI system to meet tracking accuracy requirements in practical applications [4]. In an open-loop BMI system, the movement of the external device is slowly, and introducing the visual and sensory feedback to system can overcome parts of drawbacks [4,17,18]. However, the BMI system with the visual and sensory feedback (also named simple closed-loop system in this paper) is still cannot match requirements of movement, although it is better than the open-loop system in reliability and execution speed. In order to further improve the performance of the BMI system, the auxiliary controller should be introduced to the system [2,4,5]. In this paper, considering the MPC has the following advantages: 1) the objective function can be selected in a flexible way; 2) the results of system stability and robustness can be conveniently extended to the analysis of the overall performance of the closed-loop BMI system; 3) the model and its input constraints and output constraints can be considered in one optimization problem; we use the model predictive control (MPC) strategy to design the auxiliary controller.

As early as 1990, Daniel et al. have found that intracortical micro-stimulation (ICMS) technology can affect the judgment of motion direction [19]. In recent years, the ICMS technology becomes a popular method for studying the organization of motor cortex [20,21]. The animal experiment by Sharlene et al. have shown that the ICMS can evoke the proprioceptive percepts [22]. Max et al. have designed a sensory feedback by a charge balance pulse, and good results have been obtained [23]. In the field of the BMI, Maria et al. have adopted this technology to convey the error vector of limb position to the brain, and found that this kind of feedback is effective [24]. In our previous work [2], the ICMS current was used to replace the missing proprioception feedback, and based on which a closed-loop BMI system was designed. This work had good performance of driving the artificial arm to reach the desired position, but the paper has the following two disadvantages: 1) the network of the spiking neurons used in paper [2] is time consuming although it is useful; 2) the optimization problem in [2] has 4 decision variables, hence, the optimization problem in the paper has high computational complexity.

In this paper, an improved classical SJIT model is proposed firstly, and then, a closed-loop BMI system with a Wiener-filter-based decoder, a MPC auxiliary controller and a network of Izhikevich neurons is formulated based on the improved model. In this closed-loop system, an artificial feedback is designed by the ICMS technology and the network of Izhikevich neurons; the auxiliary controller is adopted to generate the feedback information which can bring by the ICMS current. In order to simplify the computational complexity of optimization problem designed for the auxiliary control in this paper, we fixed the shape of ICMS current waveform and some of its parameters. Finally, a series of simulations are designed in this paper to show the effectiveness of the proposed measures.

2. Model improvement and performance test

2.1. The SJIT model

Fig. 1 is the SJIT model. The model shows the essential information transmission pathways for voluntary control of a single-joint

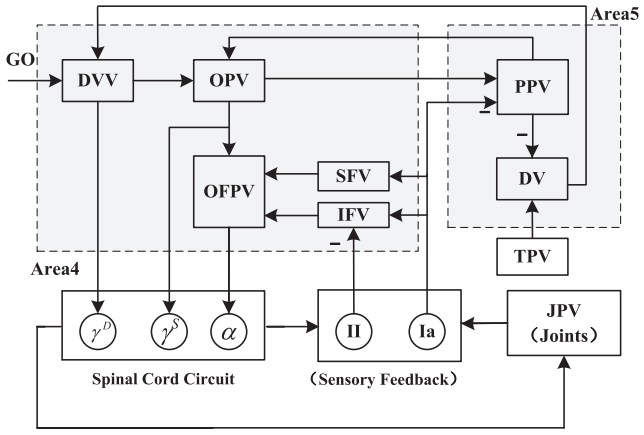

Fig. 1. The diagram has been redrawn from [10], Fig. 1.1, more details of the model can be found in [10].

(in limb) movement [10]. It should be noted that, the model can describe the qualitative relationship between cortical firing activities and joint movement clearly, although the model excludes the treatment of visual feedback during the movement. The SJIT model is briefly introduced below.

Briefly, the difference between the target and the perceived joint position vectors is computed by a population of "difference vector (DV)" neurons. The activity of these neurons is

$$r_i(t) = \max\{T_i(t) - x_i(t) + B^r, 0\}, \tag{1}$$

where $0 \le r_i(t) \le 1$ is the average firing activity of "DV" neurons related to the agonist muscle *i*. In this paper, the average firing activity of neurons related to the agonist muscle *i* is expressed by the subscript *i* and to the antagonist muscle is expressed by the subscript *j*. $T_i(t)$ represents a population of "target position vector (TPV)" neurons activity which shows the target position of the agonist muscle *i*. $x_i(t)$ represents the average firing activity of a population of "perceived position vector (PPV)" neurons which compute the present position of the agonist muscle *i* continuously. B^r is the base firing activity of the "DV" neurons.

Difference vector information is computed by the "DV" neurons continuously and then scaled by a population of "desired velocity vector (DVV)" neurons as

$$u_i(t) = \max\{g(t).(r_i(t) - r_j(t)) + B^u, 0\}, \tag{2}$$

where $u_i(t)$ is the average firing activity of a population of "DVV" neurons. B^u is the base firing activity of the "DVV" neurons. $g(t)$ is an internal "GO" signal which is assumed to be originated from the basal ganglia. "DVV" neurons fire only the process of joint movement and thus their average firing activity shows a phasic-movement time (MT) behavior. The dynamic of the internal "GO" signal is modeled as

$$\frac{dg^1(t)}{dt} = \epsilon(-g^1(t) + (C - g^1(t))g^0), \tag{3a}$$

$$\frac{dg^2(t)}{dt} = \epsilon(-g^2(t) + (C - g^2(t))g^1(t)), \tag{3b}$$

$$g(t) = g^0\frac{g^2(t)}{C}, \tag{3c}$$

where ϵ is a constant represents the slow integration rate. The constant "C" represents the saturation value of the GO signal.

The "outflow position vector (OPV)" neurons receive information from the "DVV" neurons and the "PPV" neurons, and they

show tonic firing activity. The activity of a population of "OPV" neurons is modeled as

$$\frac{dy_i(t)}{dt} = (1-y_i(t))(\eta x_i(t) + \max\{u_i(t)-u_j(t),0\}) \\ -y_i(t)(\eta x_j(t) + \max\{u_j(t)-u_i(t),0\}), \quad (4)$$

where $y_i(t)$ is the average firing rate of these neurons, and η is a scaling factor.

The average firing activity of a population of static ($\gamma_i^S(t)$) and dynamic ($\gamma_i^D(t)$) gamma motoneurons are modeled as

$$\gamma_i^S(t) = y_i(t), \quad (5a)$$

$$\gamma_i^D(t) = \rho \max\{u_i(t)-u_j(t),0\}, \quad (5b)$$

where ρ is a scaling parameter.

The average firing activity of the primary "(Ia)" and secondary ("II") muscle spindles afferents are modeled as

$$s_i^1(t) = S(\theta \max\{\gamma_i^S(t)-p_i(t),0\} + \phi \max\{\gamma_i^D(t) - \frac{dp_i(t)}{dt},0\}), \quad (6a)$$

$$s_i^2(t) = S(\theta \max\{\gamma_i^S(t)-p_i(t),0\}), \quad (6b)$$

where $s_i^1(t)$ and $s_i^2(t)$ are the primary and secondary spindles afferents average firing activity respectively. p_i is the position of the agonist muscle *i*. θ is the sensitivity of the static nuclear bag and chain fibers. ϕ is the sensitivity of the dynamic nuclear bag fibers. The saturation of spindles afferents activity is given by the function $S(\omega) = \omega/(1+100\omega^2)$.

The average firing activity $x_i(t)$ of a population of the "PPV" neurons is modeled as

$$\frac{dx_i(t)}{dt} = (1-x_i(t))\max\{\Theta y_i(t) + s_j^1(t-\tau) - s_i^1(t-\tau), \\ 0\} - x_i(t)\max\{\Theta y_j(t) + s_i^1(t-\tau) - s_j^1(t-\tau),0\}, \quad (7)$$

where τ is the delay time of the spindles feedback and Θ is a constant gain.

The average firing activity $q_i(t)$ of a population of "inertial force vector (IFV)" neurons is modeled as

$$q_i(t) = \lambda_i \max\{s_i^1(t-\tau) - s_i^2(t-\tau) - \Lambda, 0\}, \quad (8)$$

where Λ is a constant threshold. The average firing activity $f_i(t)$ of a population of "static force vector (SFV)" neurons is modeled as

$$\frac{df_i(t)}{dt} = (1-f_i(t))hs_i^1(t-\tau) - \psi f_i(t)(f_j(t) + s_j^1(t-\tau)), \quad (9)$$

where h is a constant gain which controls the strength and speed of an external load compensation, and ψ is an inhibitory scaling parameter.

The average firing activity $a_i(t)$ of a population of the "outflow force and position vector (OFPV)" neurons is modeled as

$$a_i(t) = y_i(t) + q_i(t) + f_i(t). \quad (10)$$

The average firing activity of these neurons shows a phasic-tonic behavior. The average firing activity $\alpha_i(t)$ of alpha motoneurons is modeled as

$$\alpha_i(t) = a_i(t) + \delta s_i^1(t), \quad (11)$$

where δ is a stretch reflex gain.

The joint dynamics of the arm is described by

$$\frac{d^2p_i(t)}{dt^2} = \frac{1}{K}\left(M(c_i(t)-p_i(t)) - M(c_j(t)-p_j(t)) + E_i - V\frac{dp_i(t)}{dt}\right), \quad (12)$$

where $p_i(t)$ is the position of the agonist muscle i within its range of origin-to-insertion distances. $p_j(t)$ is the position of the antagonist muscle such that $p_i(t)+p_j(t)=1$. K is the moment of inertia of the limb. V is the joint viscosity. E_i is the external force applied to the joint. $M(c_i(t), p_i(t)) = \max\{c_i(t)-p_i(t),0\}$ represents the total force generated by the agonist muscle *i*. $c_i(t)$ is the muscle contraction activity dynamics of which is given by

$$\frac{dc_i(t)}{dt} = \nu(-c_i(t) + \alpha_i(t)), \quad (13)$$

where ν scales represents the contraction rate. Since the joint is driven by muscles p_i and p_j and there exists an internal relationship between the p_i and p_j, in this paper, we only use p_i to express the joint position.

2.2. The improvement of SJIT model

The psychophysiological cortical circuit model for voluntary movement can be seen as a system. In this system, the brain is the controller, the joint position is the output of system. The SJIT model has the large overshoot which will not happen in the actual voluntary movement, the simulations in Section 4 also confirm this problem. Thus, it is necessary to improve the model. Here, we introduce the "target velocity vector (TVV)" neurons, the "joint velocity vector (JVV)" neurons and "the relative velocity vector (RVV)" neurons to improve the SJIT model.

As Fig. 2 shown, the dashed lines show the added information channels. The "TPV" and "JPV" neurons sense the information of the positions, and deliver the related information to "TVV" and "JVV" neurons, which can translate the positional information to the velocity information. "RVV" neurons accept the velocity information and then translate it to the relative velocity vector of the joint, and then, the relative velocity vector and the difference vector from "DV" neurons are combined and scaled by "DVV" neurons.

The model of "TVV" neurons and "JVV" neurons are given as

$$v_i^t(t) = \frac{dT_i(t)}{dt}, \quad v_i^p(t) = \frac{dp_i(t)}{dt}, \quad (14)$$

where the $v_i^t(t)$ is the average firing rate of "TVV" neurons, $v_i^p(t)$ is the average firing rate of "JVV" neurons. The average firing activity $v_i^r(t)$ of a population of the "RVV" neurons is modeled as

$$v_i^r(t) = \zeta(v_i^t(t) - v_i^p(t)). \quad (15)$$

where the ζ is the compensation coefficient of "RVV". In the improved model, the average firing rate of "DVV" neurons is described as follow:

$$u_i(t) = \max[g(t)(r_i(t) - r_j(t) + v_i^r(t) - v_j^r(t)) + B^u, 0]. \quad (16)$$

The introducing of "TVV","JVV","RVV" refers to the differential item of the PID control. An important reason for system overshoot is that the system has a large lag factor, and the "advance" of differential terms can largely offset the influence of lag factor. Meanwhile, the study [11] has also found that the velocity, an "advance" of differential term, should be considered in the movement model. Thus, we introduce the velocity vector in this system to reduce the overshoot. We test the performance of the improved model in Section 4.

3. The formulation of closed-loop system

From Fig. 2, we can know that the commands generated by "DVV", "OPV" and "OFPV" neurons in brain area 4 can only be executed after being transmitted by the spinal circuit, and the "PPV" neurons receive the position feedback information depend on "Ia" and "II". In the physical system of the user of artificial arm, both of above two information transmission channels need to be rebuild.

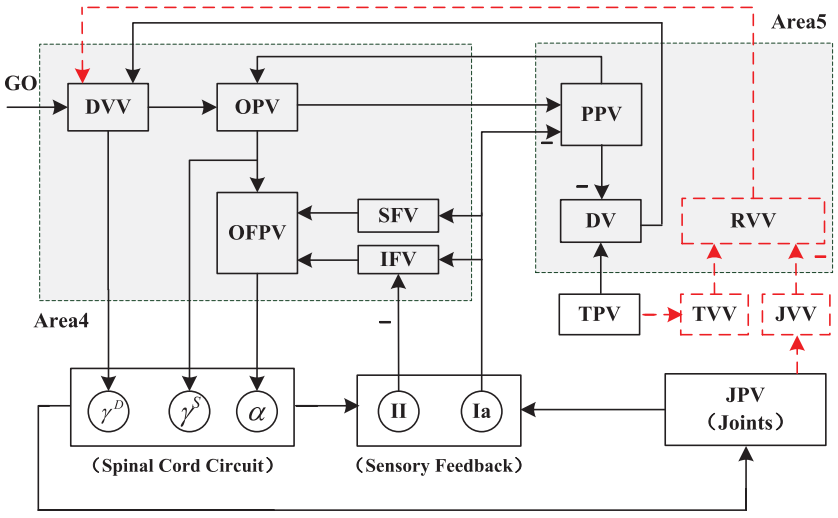

Fig. 2. The improved model.

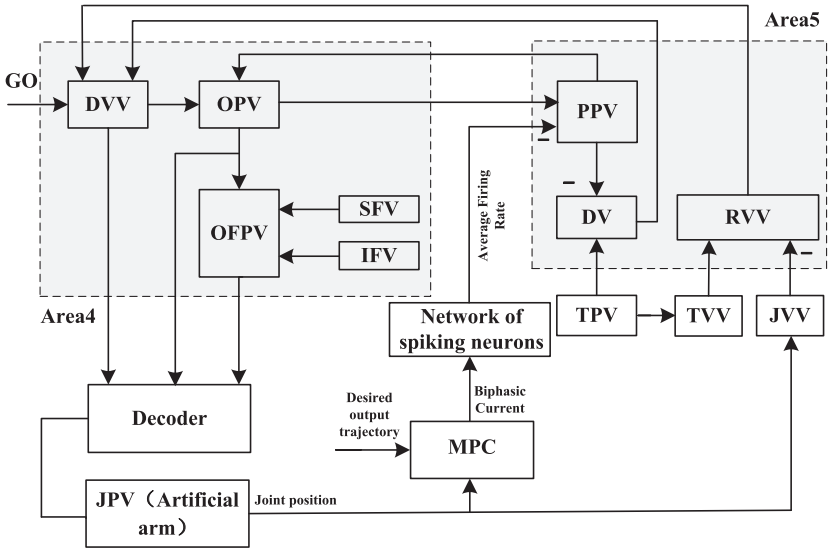

Fig. 3. The designed closed-loop BMI system.

In order to compensate the absent information channel, a closed-loop BMI system shown in Fig. 3 is formulated. In this system, the decoder is used to compensate for the absent spinal circuit, the auxiliary controller is used to generate the feedback information which can be carried by ICMS current, and the network of spiking neurons is used to encode the feedback information to average firing rate. Finally, the encoded feedback information is delivered to the "PPV" neurons.

Since ICMS technology has been widely used in deep brain stimulation, this paper uses a biphasic charge-balance waveform of current to carry the information. A network of Izhikevich neurons is introduced into the closed-loop BMI system to transform the ICMS current into the average firing rate. The auxiliary controller is designed based on the MPC strategy. The introduction of the auxiliary controller will improve the effect of recovery the motor function of arm [2]. This system is similar with the closed-loop BMI system formed in the paper [2], but the model used in this paper is the improved model and the used network of the neurons is more efficient with time. The optimization problem designed in this paper contains only one decision variable, which greatly reduces the computational complexity compared with the optimization problem in the paper [2]. It should be noted that the feedback information to the population of "IFV" and "SFV" neurons are not considered in [2] and this paper.

3.1. Decoder design

In our previous work, we have designed several decoders, and found that the decoder based on Wiener filter had the better performance [25]. In this paper, we also use this decoder to decode the information from cerebral cortex. In the process of decoder design, only the process of data collection is different from that of previous one. A brief description of data generation is given below.

During data collection, 1600 independent trials of the voluntary single-joint extension task are simulated. g^0 is modeled as a Gaussian distributed random variable with mean 0.75 and variance 0.0025 in these trials. In each trial, the simulation is performed for 3.00 s, which includes a position holding period. It should be noted that g^0 is a constant for a given trial.

In the simulation, the sampling time is selected as 10 ms. The data set including the average firing activity of population of "DVV", "OPV", "OFPV" neurons and the total force difference

is collected by (1), (3)–(13), (14)–(16). With this, a data set with 480, 000 samples is created to train the decoder.

3.2. Auxiliary controller design

In this paper, an auxiliary controller based on the MPC strategy is designed to generate the ICMS current to the networks of spiking neurons. By this way, the auxiliary control is added in the BMI system.

Briefly, when determining the control inputs, the MPC strategy can explicitly incorporate the constraints of system. When $k \geq 1$, the system model is used to predict the future outputs $p_i(k+m+1 \mid k)$ $(m = 0, 1, 2, \ldots, N_p - 1)$ which is a function of current and future control inputs $I_c(k+l \mid k)$ $(l = 0, 1, 2, \ldots, N_c - 1)$. N_p is the prediction horizon. Using these predictions, controlling inputs $I_c(k|k), I_c(k+1|k), \ldots, I_c(k+N_c-1|k)$ are computed by minimizing the cost function $\mathbb{J}_p(k)$ at sampling time k, N_c is the control horizon. Only the first computed input $I_c(k|k)$ is applied to compute the system outputs. At the step $k+1$, the optimization problem is solved again with new measurements [26,27].

The optimization problem is formulated as:

$$\min_{I_c(k|k), I_c(k+1|k), \cdots, I_c(k+N_c-1|k)} \mathbb{J}_p(k)$$

$$= \sum_{m=0}^{N_p-1} [(p_i^*(k+m+1 \mid k) - p_i(k+m+1 \mid k)]^2 \tag{17a}$$

$$\text{s.t. } (1), (3)-(4), (8)-(10), (12), (14)-(16), (18)-(20) \tag{17b}$$

$$(15) \text{ in} \tag{17c}$$

[28],

$$I_c(k+l|k) \in [0, 5000] \quad for \quad 0 \leq l \leq N_c - 1, \tag{17d}$$

$$I_c(k+l|k) = 0 \quad for \quad N_c \leq l \leq N_p - 1, \tag{17e}$$

where $I_c(k|k), I_c(k+1|k), \ldots, I_c(k+N_c-1|k)$ are the control inputs solved at the time k. In this paper, the control input $I_c(k|k)$ is used as the frequency of the ICMS current at time k. $\mathbb{J}_p(k)$ is the cost function. $p_i^*(\cdot)$ is the desired position of the agonist muscle. $p_i(\cdot)$ is the output position of the agonist muscle.

Note that: in the optimization, the continuous time t in (1),(3),(4),(8)–(10),(12),(14)–(16),(18)–(20) can be transformed into discrete time k through a sampling operation.

3.3. Network of izhikevich neurons

The typical biphasic waveform of charge-balanced ICMS current is adopted in this paper to deliver the information to the brain. The experiment made by Joseph et al. confirms that the cortical perception threshold of electrical stimulation in the range of 30–80 μA [29]. The stimulation current with the width 100 μs/phase is the "gold standard" for neurostimulation devices [24]. Hence, the 70 μA and 100 μs/phase are chosen as the amplitude and the phase width of ICMS current (Fig. 4). The frequency of ICMS current can be computed through (17).

The "PPV" neurons cannot accept the ICMS current directly. Thus, the model of spiking neurons should be introduced as a bridge between the ICMS current and the "PPV" neurons. The spiking neurons can transform the ICMS current into the average firing rate. Considering the single neuron is not representative, we formulate the spiking network with 1000 neurons through randomly

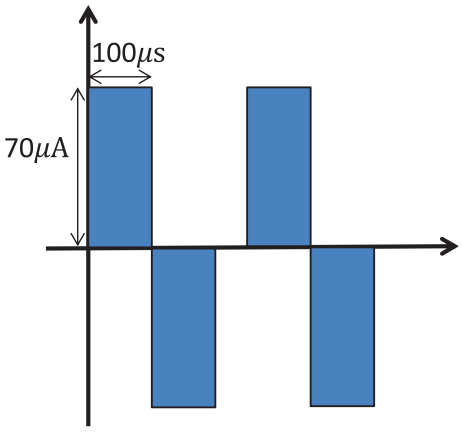

Fig. 4. The stimulation current.

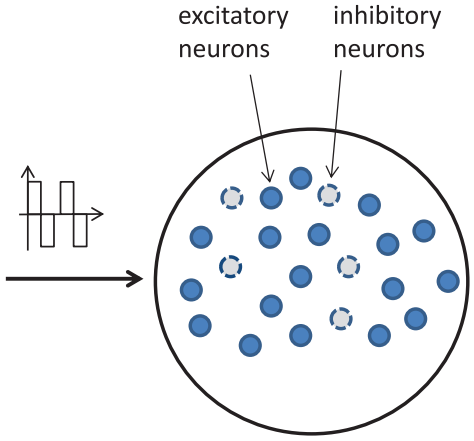

Fig. 5. The network of Izhikevich neurons.

connected weights. The ratio of the inhibitory neurons to excitatory neurons in the network is 1–4. The single neuron model in this network is proposed by Izhikevich in paper [30]. In order to make the statement of this model more concise, in this paper, we call it Izhikevich neuron model. This model can express the neuron activity vividly. This network is shown in Fig. 5, the gray circles with dashed contour represent inhibitory neurons, and the blue circles with solid contour represent excitatory neurons.

The Izhikevich neuron model is as follows [30]:

$$\dot{v} = 0.04v^2 + 5v + 140 - u + I, \tag{18}$$

$$\dot{u} = a(bv - u), \tag{19}$$

if $v \geq v_t$ mV, then $\begin{cases} v \leftarrow c \\ u \leftarrow u + d \end{cases}$, where v and u are dimensionless variables, and a, b, c, d are dimensionless parameters. v is the membrane potential of neuron. u is the membrane recovery variable. $v_t = 30$ is the firing threshold, the firing rate is the times of v reached v_t in unit time [31]. f_t is the average firing rate of these neurons. I is the injected current which consist of the ICMS current and the synaptic current. We should pay attention to a fact that each neuron in the network receives the same ICMS current.

When the average firing rate f_t is acquired, the (7) will be replaced as follow:

$$\frac{dx_i(t)}{dt} = (1 - x_i(t)) \max\{\Theta y_i(t) - f_t, 0\} - x_i(t) \max\{\Theta y_j(t) + f_t, 0\}. \tag{20}$$

3.4. Overall algorithm

The overall algorithm is given as follows:
Algorithm 1: Offline stage, for $k = 0$,

1. give the parameters of improved model, and calculate the desired position trajectory $p_i^*(\cdot)$ by (1), (3)–(16);
2. give the parameters N_p and N_c of the model predictive controller;
3. give the parameters of the formulated BMI system and simulation step $k_{\max}$.

Online stage, for each $k > 0$,

1. get the initial point $I_c(0)$ satisfied the constraint;
2. calculate $p_i(k|k), p_i(k+1|k), p_i(k+m|k), \ldots, p_i(k+N_p-1|k)$ and the cost function $\mathbb{J}_p(k)$ for each input, use the "sqp" algorithm to find the minimum value of $\mathbb{J}_p(k)$ and the $I_c(k|k), I_c(k+1|k), \ldots, I_c(k+N_c-1|k)$;
3. generate the ICMS current according to the control input $I_c(k|k)$ and other related parameters;
4. transmit the ICMS current to the network of spiking neurons to get the average firing rate f_t ;
5. impose f_t, and acquire the output of system, if $k = k_{\max}$, terminate the program; else $k = k+1$, and go to step 1.

4. Simulations

We use the matlab R2015a for the following simulations. In this section, 1) we test the improved model by comparing a series of indicators of the improved model and the SJIT model in the following two cases, namely, T_i is constant and T_i is changing; 2) the time consumption of the Izhikevich neuron network used in this paper and the neuron network used in [2] during the converting is calculated and compared through 1000 trails. 3) the formulated BMI system is tested by analyzing the performance of the system in a special reaching task.

4.1. The test of improved model

In this test, the sampling time is chosen as 10ms. During the first 50 ms, the system is in a initiating state, thus, the value of g^0 during this time is 0. The initial value of variables in the SJIT model and the improved model are set to 0 except for $x_i(0) = x_j(0) = 0.5$, $y_i(0) = y_j(0) = 0.5$, $p_i(0) = p_j(0) = 0.5$, $u_i(0) = u_j(0) = B^u$ and $r_i(0) = r_j(0) = B^r$. The parameters in the simulation are chosen as follows: $K = 200$, $V = 10$, $\nu = 0.15$, $B^r = 0.1$, $B^u = 0.01$, $\Theta = 0.5$, $\theta = 0.5$, $\phi = 1$, $\eta = 0.7$, $\rho = 0.04$, $\lambda_1 = 150$, $\lambda_2 = 10$, $\Lambda = 0.001$, $\delta = 0.1$, $C = 25$, $\epsilon = 0.05$, $\psi = 4$, $h = 0.01$ and $\tau = 0$.

Case 1: when T_i is constant during the movement process, we can find that the output of "TVV" is 0 from (14). At the same time, when $\zeta = 0$, the improved model is the same as the SJIT model. Hence, ζ is an important non-zero unknown parameter in the improved model.

First of all, we determine the parameter ζ by studying dynamic indicators of the system with different ζ. Table 1 shows dynamic indicators of the system in the case of $T_i = 0.7, g^0 = 0.75$ with different ζ. In Table 1, t_r is the rise time, t_p is the peak time, σ is the overshoot of system. The qualitative relationship is easy to be obtained, although the results in this table cannot provide a clear quantitative relationship. With the increasement of ζ, the overshoot σ decreases gradually. For example, in the case of $\zeta = 5$, the overshoot of improved model is 0.60% lower than that of the SJIT model.

Considering the above system performance indicators, set $\zeta = 1$. Under this circumstance, the tracking results of the improved model and the SJIT model are shown in Fig. 6. It can be clearly seen from the figure that compared with the SJIT model, the overshoot of the improved model is greatly reduced. However, it should be noted that these decrements are at the cost of increasing response time.

Table 1
The dynamic indicators of improved model ($g^0 = 0.75, T_i = 0.7$).

No.	ζ	t_r(ms)	t_p(ms)	σ
1	0.0	460	650	0.75%
2	0.5	460	680	0.59%
3	1.0	470	740	0.46%
4	1.5	480	790	0.44%
5	2.0	490	830	0.42%
6	2.5	500	850	0.41%
7	3.0	510	860	0.38%
8	3.5	520	880	0.35%
9	4.0	540	890	0.28%
10	4.5	550	910	0.19%
11	5.0	570	1250	0.15%

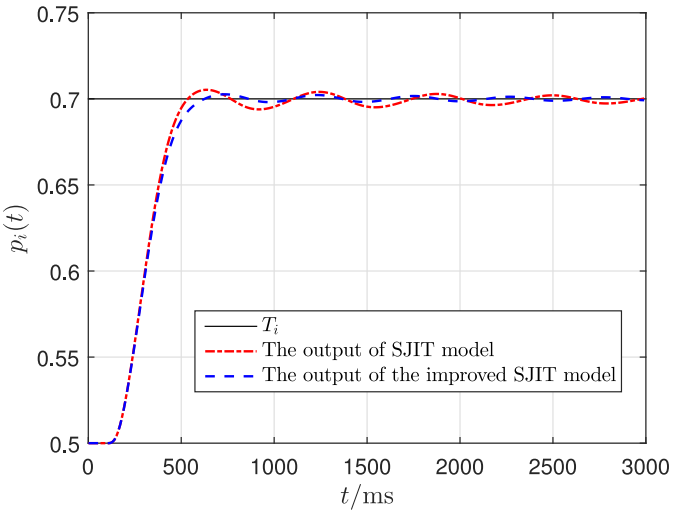

Fig. 6. The tracking results of static trajectory ($T_i = 0.7, g^0 = 0.75, \zeta = 1$).

Table 2
The comparison of dynamic indicators.

No.	g_0	The origin model			The improved model		
		t_r(ms)	t_p(ms)	σ	t_r(ms)	t_p(ms)	σ
1	0.35	910	1280	0.81%	920	1350	0.51%
2	0.45	740	1080	0.88%	760	1120	0.62%
3	0.55	610	940	0.87%	630	980	0.68%
4	0.65	510	800	0.66%	530	870	0.63%
5	0.75	460	650	0.75%	470	740	0.38%
6	0.85	430	580	1.49%	440	600	0.67%
7	0.95	410	550	2.27%	420	560	1.40%

Next, the dynamic indicators of the improved model with different GO signals (g^0) are tested. Table 2 gives the comparison results. From Table 2, it can be seen that σ of the improved model is lower than SJIT model under all given cases, and the value of σ is minimum when $g^0 = 0.75$. Thus, g^0 is set to this value in subsequent simulations. Of course, the reduction of overshoot is also achieved by sacrificing the response time of system.

Case 2: when T_i is changing during the movement process, 12 dynamic target trajectories shown Table 3 are chosen: the initial position of these trajectories are chosen as 0.7, 0.5 and 0.4, and the initial velocity as $\pm$ 0.1/s, $\pm$ 0.2/s, $\pm$ 0.3/s. In all trajectories, the position remained unchanged after the first 1 s. The mean absolute scaled error (MASE) [32] and sum of squared er-

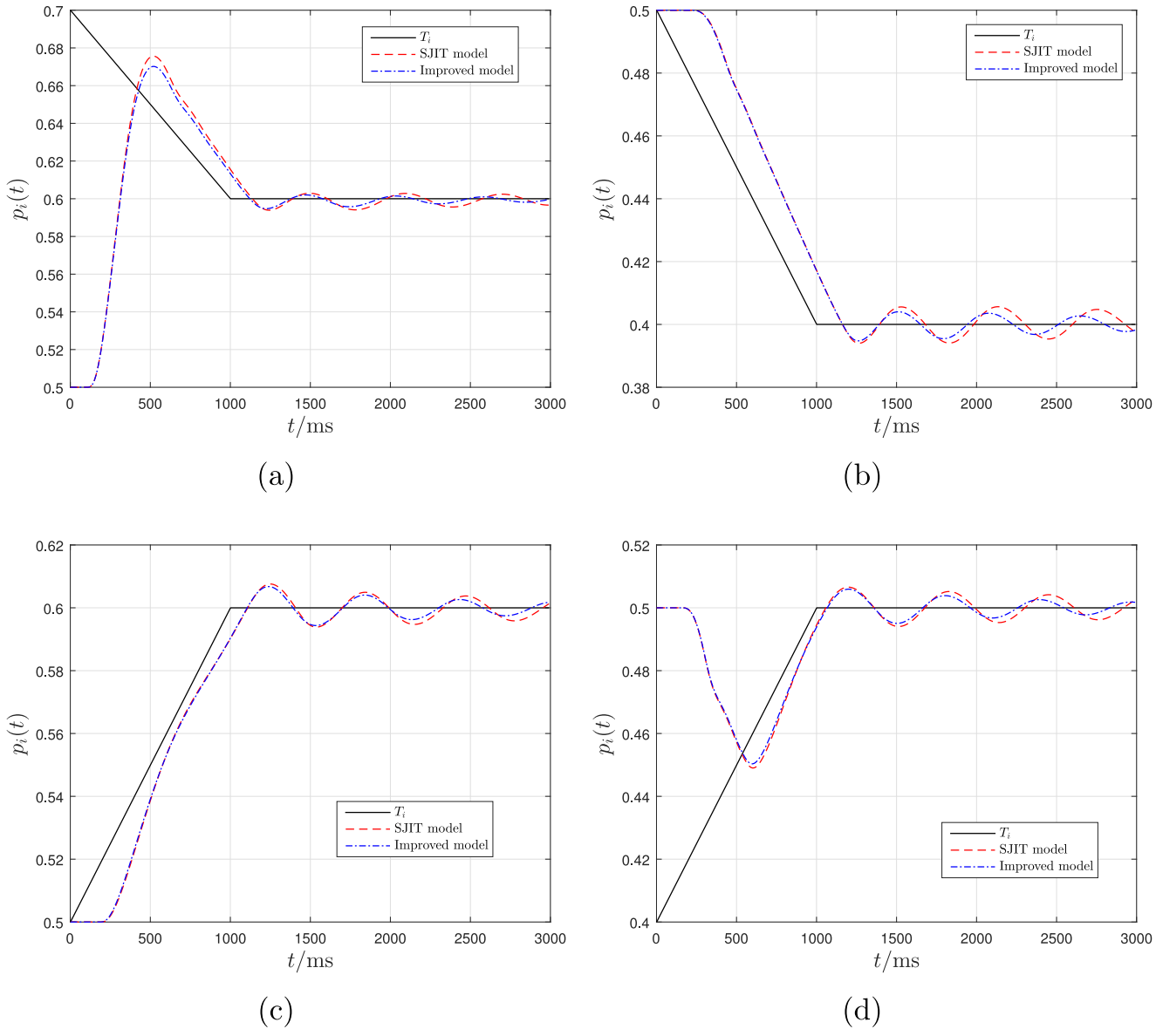

Fig. 7. The tracking results under different dynamic target trajectories: (a), (b), (c) and (d) show the results of No. 1, 4, 9 and 12 in Table 3, respectively.

ror (SSE) between the system output trajectories $p_i(t)$ and the dynamic target trajectories of T_i are used to evaluate the tracking effect. The test results are also shown in Table 3 and Fig. 7. It can be seen from Table 3 that, in all 12 target trajectories, the MASE and SSE of improved model are both smaller than that of SJIT model. Fig. 7 shows several tracking results under the target trajectories with No. 1, 4, 9 and 12 in Table 3, respectively, and it is clear that the tracking performance of improved model is better than that of SJIT model.

4.2. The comparison of neuron networks

The sampling time is selected as same as that in Section 4.1. The constant parameters of the Izhikevich neurons network are as follows: each excitatory neuron has $(a_n, b_n) = (0.02, 0.2)$ and $(c_n, d_n) = (-65 + 15r_n^2, 8 - 6r_n^2)$, where r_n is a random variable belong to [0, 1] and i is the neuron index. Similarly, each inhibitory neuron has $(a_n, b_n) = (0.02 + 0.08r_n, 0.25 - 0.05r_n)$ and $(c_{ni}, d_n) = (65, 2)$. As in [30], the synaptic connection weights belong to [0, 0.5]. We set the amplitude and the frequency of the ICMS as 70μA and 5000Hz, respectively.

We give the generated current to the Izhkevich neuron network and the neuron network in [2], and calculate the time consumption of converting the ICMS current into average firing rate, respectively. In this paper, 1000 experiments are carried out and the average time of the process is calculated. The experimental results show that,the average conversion time of the network of Izhikevich neurons used in this paper is 0.056 s and that of the neurons network used in [2] is 34.696 s. It can be seen that the neurons network adopted in this paper has better time efficiency.

4.3. The closed-loop BMI system performance

In this simulation, the formulated closed-loop BMI system performance is tested. In this test, T_i is selected as No.1 in Table 3, the target trajectory p_i^* is obtained by the improved model. The parameters of MPC controller are chosen as: $N_p = 30$, $N_c = 5$. The sampling time and the initial state are the same as that proposed

Table 3
The tracking results under different dynamic target trajectories.

No.	Dynamic trajectory		MASE		SSE	
	initial position	initial velocity	SJIT model	improved model	SJIT model	improved model
1	0.7	-0.1	71.9878	68.4234	0.9108	0.9051
2	0.7	-0.2	49.4848	46.9500	0.9956	0.9653
3	0.7	-0.3	47.7465	45.6943	1.4928	1.4349
4	0.5	-0.1	27.8731	25.8326	0.0504	0.0482
5	0.5	-0.2	42.0443	41.3201	0.4831	0.4767
6	0.5	-0.3	56.9049	56.3808	1.7779	1.7585
7	0.5	+0.3	21.0355	20.7739	0.3044	0.3014
8	0.5	+0.2	19.3387	18.4436	0.1022	0.0999
9	0.5	+0.1	18.0849	16.6629	0.0199	0.0184
10	0.4	+0.3	19.2574	18.6157	0.2993	0.2606
11	0.4	+0.2	23.6148	22.5107	0.2514	0.2270
12	0.4	+0.1	41.8949	40.1223	0.2433	0.2126

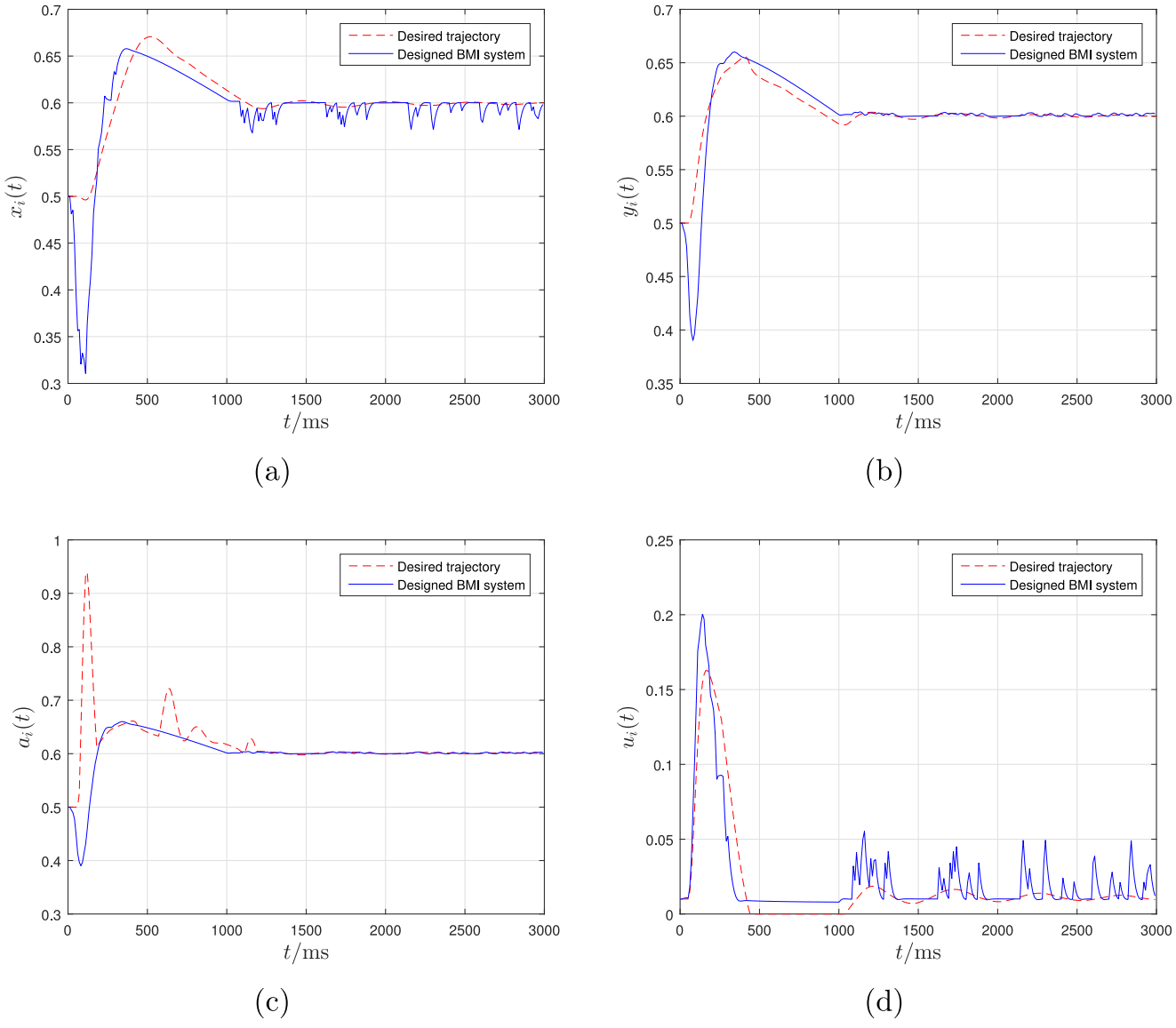

Fig. 8. The comparisons of the average firing rates.

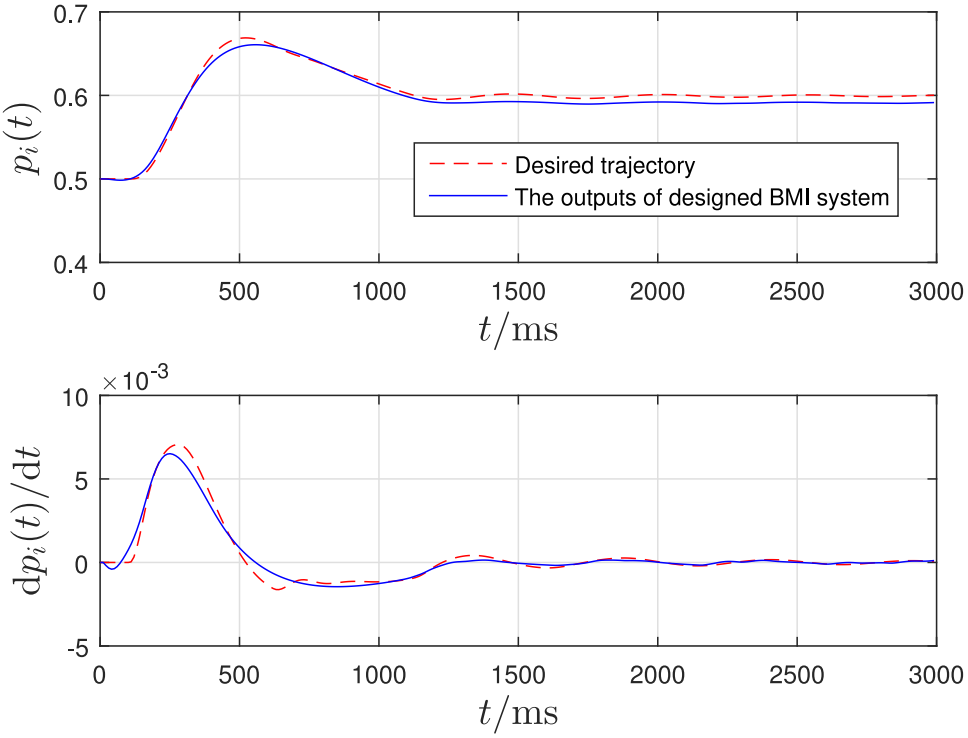

Fig. 9. The effect of joint motor function recovery.

in the Section 4.1. The parameters of the Izhikevich neurons network are same as that in the Section 4.2.

Fig. 8 shows the comparisons of "x_i","y_i","a_i","u_i" in the closed-loop BMI system and in the desired case (voluntary movement). Fig. 9 shows the position tracking results of the closed-loop BMI system designed in this paper. From these figures, we can find that the designed system can track the desired position trajectory well, although there are some errors in the recovery of average firing rates of neurons population in cerebral cortex, that is, the designed BMI system can recover the motor function of the joint well.

4.4. Further discussions

(1) Discussion about the improved model. From the perspective of system modelling, the improved SJIT model proposed in this paper can reduce the system overshoot by introducing "TVV", "JVV" and "RVV" neurons. Considering the overshoot does not really exist in human voluntary motion, hence, the proposed model solves the mismatch problem in some extent. From the perspective of application, when we design the BMI system based on the proposed model, the desired joint trajectory would have a little oscillation, which can reduce the difficulty of tracking the desired trajectory. For example, if the manipulator is controlled to track the desired trajectory with large oscillation, the mechanical wear of manipulator will increase.

(2) Discussion about the designed BMI system. In this paper, an auxiliary controller is introduced to formulated closed-loop BMI system. This strategy can improve the tracking effect greatly and give the guidance to the design of BMI system with improved performance. The MPC control strategy adopted in this paper not only has high control accuracy, but also can take the physical constraints into account in the control process, which can provide security for the BMI system. However, each step of control requires solving an optimization problem, which increases the computational burden of the system. In this paper, the calculation complexity of the optimization problem is greatly reduced by fixing the amplitude and width of ICMS current; in addition, the used Izhikevich neuron network in the BMI system has high time efficiency, which can also speed up the execution of BMI system.

(3) Discussion about the undershoot. In the process of joint movement, the trajectories of "x_i", "y_i", "a_i" (see Fig. 8) in the formulated closed-loop BMI system contain undershoots near the time 0, which are caused by the auxiliary controller, i.e., to track the target position trajectory quickly, the auxiliary controller must calculate the input with large amplitude and implement the input to system. Of course, we can reduce the undershoot through shrink the input constraints, but the tracking time will be lengthened.

5. Conclusions

In this paper, an improved psychophysiological cortical circuit model for single-joint movement is proposed; then, based on the improved model, a closed-loop BMI system is formulated. In the system, a Wiener filter-based decoder is used to compensate for the absent spinal circuit, an artificial feedback to the brain is designed based on the charge-balanced ICMS current and the Izhikevich neurons network, and an auxiliary controller is designed to assist the controlling of artificial arm through generating the feedback information which can be brought by the ICMS current. Through the simulations, we find that 1) the improved model can reduce the large overshoot deficiency of SJIT model and it is closer to the true single-joint movement; 2) the Izhikevich neurons network used in this paper is more time efficient than the existing one; 3) the closed-loop system designed in this paper is efficacious to track the desired position trajectory.

Declaration of Competing Interest

We declare that we do not have any commercial or associative interest that represents a conflict of interest in connection with the work submitted.

References

[1] M.M. Shanechi, A.L. Orsborn, H.G. Moorman, S. Gowda, S. Dangi, J.M. Carmena, Rapid control and feedback rates enhance neuroprosthetic control, Nat. Commun. 8 (2017) 13825.

[2] H. Pan, B. Ding, W. Zhong, G. Kumar, Designing closed-loop brain-machine interfaces with network of spiking neurons using MPC strategy, in: American Control Conference, 2016, pp. 2543–2548.

[3] I. Iturrate, J.M. Antelis, A. Kubler, J. Minguez, A noninvasive brain-actuated wheelchair based on a p300 neurophysiological protocol and automated navigation, IEEE Trans. Rob. 25 (3) (2009) 614–627.

[4] A. Orsborn, Closed-Loop Design of Brain–Machine Interface Systems, UC Berkeley, 2013 Ph.D. thesis.

[5] N.S. Davidovics, G.Y. Fridman, B. Chiang, C.C.D. Santina, Effects of biphasic current pulse frequency, amplitude, duration, and interphase gap on eye movement responses to prosthetic electrical stimulation of the vestibular nerve, IEEE Trans. Neural Syst. Rehabilit. Eng. 19 (1) (2011) 84.

[6] M.H. Shi, C.L. Zhou, J. Xie, S.Z. Li, Q.Y. Hong, M. Jiang, F. Chao, W.F. Ren, X.Q. Liu, D.J. Zhou, Electroencephalogram-based brain-computer interface for the chinese spelling system: a survey, Front. Inf. Technol. Electron. Eng. 19 (3) (2018) 423–436.

[7] T. Suyama, A network-type brain machine interface for supporting activities of daily living, in: ACM International Joint Conference on Pervasive and Ubiquitous Computing and Proceedings of the 2017 ACM International Symposium on Wearable Computers, 2017, pp. 1930–1937.

[8] E. Hortal, D. Planelles, F. Resquin, J.M. Climent, J.M. Azorn, J.L. Pons, Using a brain–machine interface to control a hybrid upper limb exoskeleton during rehabilitation of patients with neurological conditions, J. Neuroeng. Rehabilit. 12 (1) (2015) 1–16.

[9] F. Filimon, Human cortical control of hand movements: parietofrontal networks for reaching, grasping, and pointing, Neurosci. Rev. J. Bring. Neurobiol. Neurol. Psychiatry 16 (4) (2010) 388.

[10] D. Bullock, P. Cisek, S. Grossberg, Cortical networks for control of voluntary arm movements under variable force conditions, Cerebral Cortex 8 (1) (1998) 48–62.

[11] E. Todorov, Direct cortical control of muscle activation in voluntary arm movements:a model, Nat. Neurosci. 3 (4) (2000) 391–398.

[12] S. Shoham, L.M. Paninski, M.R. Fellows, N.G. Hatsopoulos, J.P. Donoghue, R.A. Normann, Statistical encoding model for a primary motor cortical brain–machine interface, IEEE Trans. Biomed. Eng. 52 (7) (2005) 1312–1322.

[13] B. Pollok, J. Gross, A. Schnitzler, How the brain controls repetitive finger movements, J. Physiol.-paris 99 (1) (2006) 8–13.

[14] R. Esposti, P. Cavallari, F. Baldissera, Feedback control of the limbs position during voluntary rhythmic oscillation, Biol. Cybern. 97 (2) (2007) 123–136.

[15] G. Kumar, M.H. Schieber, N.V. Thakor, M.V. Kothare, Designing closed-loop brain-machine interfaces using optimal receding horizon control, in: American Control Conference, 2013, pp. 5029–5034.

[16] F. García-Córdova, A cortical network for control of voluntary movements in a robot finger, Neurocomputing 71 (1) (2007) 374–391.

[17] S. Dangi, S. Gowda, R. Heliot, J.M. Carmena, Adaptive kalman filtering for closed-loop brain-machine interface systems, in: International IEEE/EMBS Conference on Neural Engineering, 2011, pp. 609–612.

[18] D. Sussillo, P. Nuyujukian, J.M. Fan, J.C. Kao, S.D. Stavisky, S. Ryu, K. Shenoy, A recurrent neural network for closed-loop intracortical brain–machine interface decoders, J. Neural Eng. 9 (2) (2012) 026027.

[19] C.D. Salzman, K.H. Britten, W.T. Newsome, Erratum: cortical microstimulation influences perceptual judgements of motion direction, Nature 346 (6284) (1990). 589–589

[20] M.K. Baldwin, D.F. Cooke, L. Krubitzer, Intracortical microstimulation maps of motor, somatosensory, and posterior parietal cortex in tree shrews (tupaia belangeri) reveal complex movement representations, Cerebral Cortex 27 (2) (2016) 1439.

[21] E.L. Stegemöller, C. Zadikoff, J.M. Rosenow, C.D. Mackinnon, Deep brain stimulation improves movement amplitude but not hastening of repetitive finger movements, Neurosci. Lett. 552 (1) (2013) 135–139.

[22] S.N. Flesher, J.L. Collinger, S.T. Foldes, J.M. Weiss, J.E. Downey, E.C. Tyler-Kabara, S.J. Bensmaia, A.B. Schwartz, M.L. Boninger, R.A. Gaunt, Intracortical microstimulation of human somatosensory cortex, Sci. Transl. Med. 8 (361) (2016) 361ra141.

[23] M. Ortizcatalan, B. Håkansson, R. Brånemark, An osseointegrated human–machine gateway for long-term sensory feedback and motor control of artificial limbs, Sci. Transl. Med. 6 (257) (2014) 257re6.

[24] M.C. Dadarlat, J.E. O'Doherty, P.N. Sabes, A learningcbased approach to artificial sensory feedback leads to optimal integration, Nat. Neurosci. 18 (1) (2015) 138–144.

[25] H. Pan, W. Mi, J. Sun, B. Ding, The decoder performance comparison in the closed-loop bmi system based on mpc, in: 2018 37th Chinese Control Conference, 2018.

[26] H. Pan, W. Mi, X. Lei, J. Deng, A closed-loop brain-machine interface framework design for motor rehabilitation, Biomed. Signal Proces. (2020), doi:10.1016/j.bspc.2020.101877.

[27] H. Pan, W. Mi, The adaptive decoder design based on the receding horizon optimization in BMI system, Cogn Neurodynamics (2020), doi:10.1007/s11571-019-09567-4.

[28] H. Pan, M. Wang, Z. Wang, P. Wang, The performance comparison of two kinds of decoders in brain-machine interface, in: International Symposium on Computer, 2016, pp. 247–250.

[29] T.J. Foutz, C.C. Mcintyre, Evaluation of novel stimulus waveforms for deep brain stimulation, J. Neural Eng. 7 (6) (2010) 066008.

[30] E.M. Izhikevich, Simple model of spiking neurons, IEEE Trans. Neural Netw. 14 (6) (2003) 1569–1572.

[31] A.M. Andrew, Spiking neuron models: single neurons, populations, plasticity, Kybernetes 4 (7/8) (2002) 277C280.

[32] R.J. Hyndman, A.B. Koehler, Another look at measures of forecast accuracy, Int. J. Forecast. 22 (4) (2006) 679–688.

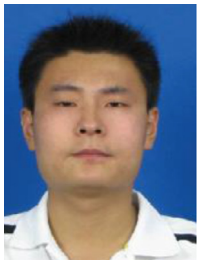

Hongguang Pan (1983–) received the bachelor's degree from the Xi'an University of Science and Technology, in 2007, and the Ph.D. degree from Xi'an Jiaotong University, in 2015. From September 2013 to March 2015, he studied in Lehigh University, USA, as a Visiting Ph.D. Student. He is a master supervisor of Xi 'an University of Science and Technology currently. His research interest covers brain-machine interface system, intelligent control and predictive control.

Wenyu Mi (1995–) She is a master's degree candidate in Xi 'an University of Science and Technology currently. Her research interest covers brain-machine interface system, model predictive control and deep learning.

Xinyu Lei (1995–) received her bachelor's degree at Xi 'an University of Science and Technology in 2017 and has been studying at Xi 'an University of Science and Technology for master's degree since 2017. Her research interest covers image classification, image segmentation, machine learning, deep learning and their applications.

Weimin Zhong (1976–) He is a doctoral supervisor of East China University of Science and Technology currently. His research interest covers machine learning, swarm intelligent algorithm and operation optimization of complex chemical production process.